Science of Friction–Adhesive Joints

Eugenio Dragoni and Pierfranco Mauri

Abstract This chapter addresses the fundamental properties of hybrid friction–adhesive joints which combine any form of mechanical tightening (stimulus for friction forces) with anaerobic adhesives. By filling the voids around the microareas of true metal-to-metal contact between the mating parts, anaerobic adhesives allow the full area involved by the engagement to be usefully exploited. Advantages ranging from sealing action, fretting suppression, noise reduction and enhanced strength derive from this combination. The focus of the chapter is on predicting the mechanical strength of these joints. The literature covering the static and the fatigue strength is reviewed showing that proper choice of the adhesive can increase the overall strength of the joint well above the strength of the purely mechanical joint based on friction only. Simple equations are also provided for the strength calculation of practical engineering assemblies.

1 Introduction

Purely mechanical joints based on the frictional forces arising at the pre-loaded contact between metal parts have become a common assembly solution in machine constructions since a long time. Anaerobic adhesives (anaerobics) are an effective

E. Dragoni (✉)
Department of Sciences and Methods for Engineering, University of Modena and Reggio Emilia, Via Amendola 2, 42122 Reggio Emilia, Italy
e-mail: eugenio.dragoni@unimore.it

P. Mauri
Henkel Italia S.p.A., Via Amoretti 78, 20157 Milan, Italy
e-mail: Piero.Mauri@it.henkel.com

Adv Struct Mater (2011) 6: 201–225
DOI: 10.1007/8611_2010_34

Published Online: 23 July 2010

means to improve the performance of these joints because they tolerate being trapped between closely matching surfaces subjected to substantial clamping forces. Threaded connections, flanged couplings, taper or interference fits (Fig. 1) are typical examples taken from the wide range of applications which benefit from these machinery adhesives [12]. A distinguished property of anaerobic adhesives is the low demand that they put on the design of the joint which in most cases can be efficiently bonded as it was conceived for the standard assembly. This characteristic represents a remarkable advantage over virtually all other types of adhesive and makes them ideal candidates to solve many problems of mechanical design.

Anaerobic adhesives belong to the large family of thermosetting acrylic polymers and are kept stable as one-part liquids by the oxygen in the air. Easily applied to the adherends by manual or automatic means, anaerobics cure when confined in the airless pockets (hence the name) left by the roughness of the mating metal surfaces upon tightening of the joint (Fig. 2). Advantages of the adhesive-augmented friction joints include added sealing action, improved corrosion resistance, reduced fretting wear and increased mechanical strength. The strength enhancement brought forth by the adhesive is comparable to (often greater than) the strength of the purely mechanical (dry) joint. This improvement results in more compact (thus cheaper) constructions when a new design is undertaken to meet a specified load-carrying capacity. Alternatively, existing designs can be upgraded at marginal costs whenever the strength expectations of the market become more demanding with time.

This chapter reviews the scientific literature dealing with the static and the fatigue strength of bonded joints based on this hybrid technology. The focus of the review is on the fundamental properties of the friction–adhesive interface rather than on applications. The technological aspects of anaerobics usage together with several representative case studies are presented and discussed in the next chapter of this book.

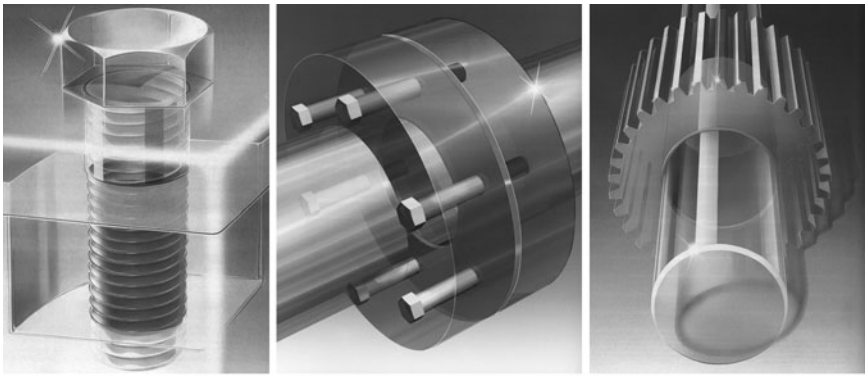

Fig. 1 Typical applications of anaerobic adhesives to complement mechanically tightened friction joints: **a** threaded connections, **b** flanged couplings, **c** cylindrical fits

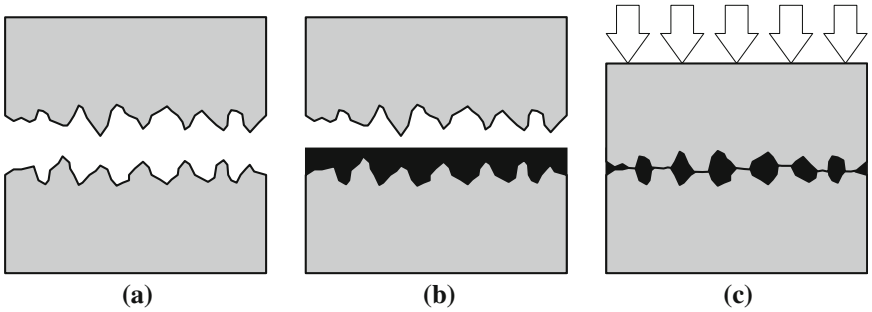

Fig. 2 The three stages of formation of a hybrid friction–adhesive joint: **a** dry joint, **b** adhesive application, **c** joint closure and tightening

Systematic research on anaerobics can be traced back to the paper by O'Reilly [19] covering static testing and design of bonded cylindrical interference-fits, a mainstay of anaerobic technology. Mahon [17] and Sawa et al. [24] demonstrated how anaerobics can be used to enhance the strength of flanged couplings. A review of anaerobics application to axisymmetric joints is given by Romanos [23] and Bartolozzi et al. [2]. Dragoni [6] showed that anaerobic threadlockers can improve the fatigue life of threaded connections by reducing the fretting damage (thus delaying crack initiation) between nut and bolt threads. The effects of bolt preload, bolt diameter, thread pitch and surface treatment on breakaway, breakloose and prevailing torques in commercial nut-bolt connections bonded with an anaerobic threadlockers were measured by Sekercioglu and Kovan [29]. Yoneno et al. [32–34], Sawa et al. [25] and Kawamura et al. [14] presented an analytical model for the stress analysis in the adhesive layer of bonded interference fits between hollow round shafts and annular hubs undergoing push-off and torsional loading. Their predictions are far on the conservative side when compared with the outcome of static tests. Dragoni and Mauri [7] investigated the intrinsic properties of friction–adhesive interfaces by torsional testing of annular butt joints subjected to controllable normal pressure. Their measurements on a single adhesive supported the conclusion that the cumulative strength of the hybrid interface equals the sum between the strength of the purely adhesive interface and the strength of the purely frictional interface for any contact pressure. By extending the investigation to an assortment of anaerobics tested both in ideal conditions (butt interface) and in real working conditions (threads, cylindrical fits and overlaps), Dragoni and Mauri [8] observed that the strength of the hybrid joints increases with the contact pressure but the superimposition of strengths (purely frictional + purely adhesive) is not always verified. More recently, a paper by Dragoni [9] evaluated the fatigue behavior of hybrid friction–adhesive tapered joints, proposing an empirical relationship between the fatigue limit and the static strength. The result can help the designer in predicting the behaviour under cyclic stresses starting from the more readily available static failure stress. Canyurt [3] used a genetic algorithm to estimate the fatigue strength of bonded tubular joints including the effect, based on

third-party results, of assembly interference between the adherends. A limited range of static and fatigue tests on bonded interference and slip fits between steel pin and collars were discussed by Sekercioglu et al. [27] and by Sekercioglu [28]. The latter paper examines the strength of slip fits using modern statistical tools of reliability-based structural design. Aiming at the optimization of front bike forks, Croccolo et al. [4] carried out static and fatigue push-off tests on bonded press-fits between steel and aluminium shafts fitted with steel bushings. They analyzed the experimental results under the common, though empirical, assumption that the overall strength of the hybrid joint equals the sum of frictional and adhesive strengths, calculated independently of each other.

By examining the above literature and particularly the papers by Dragoni [9] and Dragoni and Mauri [7, 8], this chapter has three main purposes. First, summarize the static strength of hybrid interfaces, formed from a variety of adhesives and showing both ideally regular (annular butt joints) or realistically irregular (threaded, cylindrical and double-lap joints) stress distributions over the bondline. Second, correlate the fatigue strength of the hybrid interface to the corresponding static strength from tests on bonded taper fits. Third, provide a micromechanical model of the hybrid interface and supply engineering formulae for the strength calculation of typical industrial joints.

2 Experimental Details

2.1 Static Strength of the Ideal Interface

An ideal friction–adhesive interface is a bonded interface submitted to homogeneous (uniform) contact pressure (upon joint formation) and homogeneous shear stresses (upon breakaway). Testing of these particular interfaces aims at understanding the intimate interaction between friction and adhesive forces exchanged by the bonded parts. Experiments on nearly ideal interfacial conditions were performed by Dragoni and Mauri [7, 8] using the simple device shown in Figs. 3, 4a.

The equipment in Fig. 3 realizes axisymmetric butt joint conditions according to ASTM E229. The primary engagement occurs at *x*-*x* between the annular end faces (∅30 × 37 mm) of the steel bushings 4 and 5 (quenched and drawn 39NiCr Mo3 to EN 10083-3, with ultimate tensile strength $S_u = 1{,}100$ N/mm^2 and yield strength $S_y = 850$ N/mm^2). The axial contact force is provided by the centre bolt 2 (M14 × 120, property class 12.9), tightened through the flanged nut 8 (property class 10.9). The friction between the threads of bolt and nut is kept to a minimum by smearing them with low-friction lubricating paste (Molykote G-n plus). The bolt head, angularly secured by setting screw 1, pushes on bushing 4 through quenched steel washer 3, whereas nut 8 presses on bushing 5 through collar 7 and thrust roller bearing 6 (INA 81206). The bearing serves the double purpose of limiting the torque on the annular interface upon tightening and reducing the resisting torque from outside the interface upon breakaway (see below).

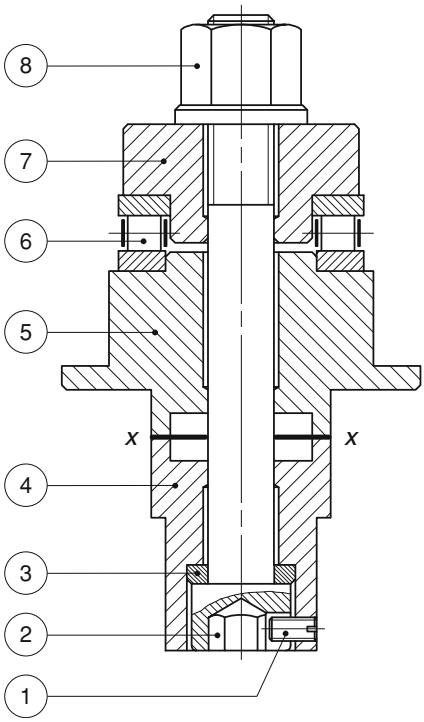

Fig. 3 Section view of the device used to produce uniform interfacial stress conditions (at *x*–*x*): (*1*) setting screw, (*2*) centre bolt, (*3*) washer, (*4*) lower bushing, (*5*) upper bushing, (*6*) roller bearing, (*7*) collar, (*8*) flanged nut

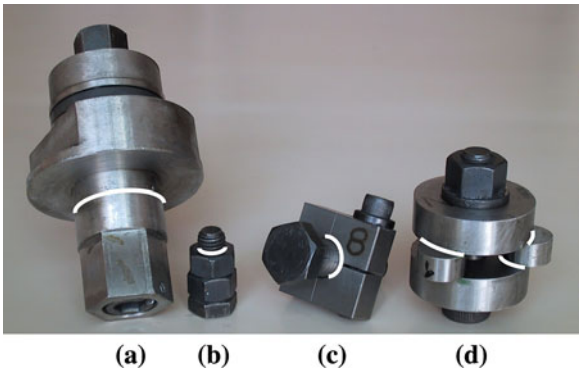

Fig. 4 Overview of the specimens used for static characterization of the hybrid friction–adhesive interface (in *white* the *bondline*): **a** ideal interface, **b** threaded connection, **c** cylindrical fit, **d** double-lap joint

The tightening and the breakaway operations are simplified by lateral flats machined on bushings 4 and 5 to allow fixation in a vice and torque application with a wrench (Fig. 4a). Although designed to be cheap (no expensive load cells) and simple to use (hand operated), the described device ensures ideal working conditions at the interface. First of all, the flat active surfaces facilitate cleaning, treatment and closure of the joint. In the second place, the narrow annular shape transfers constant pressure under the closing force and nearly uniform shear stresses under the breakaway torque. In particular, the bondline is free from stress singularities which

are an inherent feature at the edges [1] of more common specimens like the overlap joint [21], the pin-collar coupon [11] and many others [16].

The tests with the device in Fig. 3 were carried out in four steps as follows:

1. *Surface preparation*: removal of adhesive residuals (if any) and manual regeneration of surface roughness to $Ra = 0.8–1.2$ μm on flat sanding table (grit size P60), followed by check of the planarity of the surface (hand adjustment with file, if necessary) and final degreasing with liquid trichloroethane.
2. *Assembly and preloading*: fixation of bushing 4 in a vice, application of anaerobic adhesive (if necessary), assembly of specimen and tightening of nut 8 under prescribed torque (electronic wrench) to apply a specific contact force according to an experimentally determined torque-preload calibration curve (see [7]).
3. *Consolidation of interface*: permanence in oven at 40°C for 8 h (curing of adhesive) and subsequent acclimatisation in still air at room temperature (20°C) for about 12 h for complete growth of metal junctions between roughnesses [30]).
4. *Breakaway*: blocking of bushing 5 in a vice and gradual application of torque (electronic wrench) to bushing 4 up to fracture of the interface. The maximum (breakaway) torque recorded by the wrench less the small friction torque of the roller bearing 6 at the applied axial load (see [7]) gives the torsional strength of the interface.

The investigation by Dragoni and Mauri [7, 8] involved the products Loctite 638, 601, 243, 242 and 222. These products span the full range of anaerobics in terms of mechanical strength and field of application. Loctite 638 is a high-strength retainer, particularly suited for permanent cylindrical fits. Loctite 601 is a medium/high-strength retainer, tailored for cylindrical joints and general purpose bonding. Loctite 243, 242 and 222 are medium- and low-strength threadlockers, used to prevent rotation and conserve preload in threaded joints.

Along with the bonded interfaces, the tests included a number of unbonded assemblies, tightened under a variety of loads, to gain information on the strength of the dry interface. All tests were performed on twelve identical devices as in Fig. 4a, which were used to carry out sequential runs of twelve different test conditions, randomly allocated to the specimens.

2.2 Static Strength of Real Joints

For the tests carried out under realistic working conditions, Dragoni and Mauri [8] examined three joint geometries: threaded connections (Fig. 5a), cylindrical fits (Fig. 5b) and double-lap joints (Fig. 5c). Pictures of these specimens are shown in Fig. 4b–d, next to the device used to achieve ideal interface conditions. A description of the joints and of the testing procedure follows.

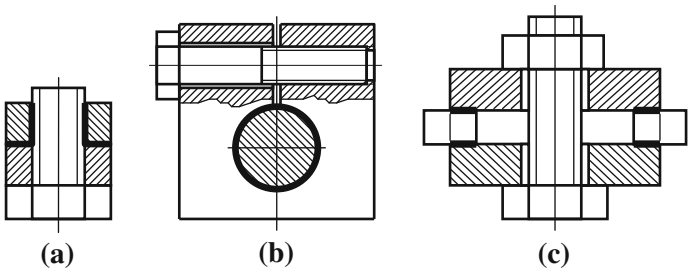

Fig. 5 Joint geometries providing realistic interface conditions: **a** threaded connection, **b** cylindrical fit, **c** double-lap joint (*bondline* shown with *heavy lines*)

1. *Threaded connections*. The threaded connection in Fig. 5a comprises a commercial M12 × 30 steel bolt (grade 8) and two commercial M12 × 10 steel nuts (grade 8). Bolt and nuts were initially degreased by repeated soaking in liquid trichloroethane. After that, each sample was assembled by driving the lower nut against the head of the bolt followed by controlled tightening of the upper nut, with adhesive applied (if any) to both thread and bearing face. Permanently engaged with the incomplete thread turns underneath the bolt head, the first nut provides a neat countersurface for the second nut which embodies the actual test piece. Details on the conversion of the tightening torque applied to the upper test nut into effective preload induced in the bolt are provided by Dragoni and Mauri [8]. The strength measurements were performed by recording with an electronic wrench the peak torque required to unscrew the top nut after consolidation of the interface. Due to the difficulty in restoring the working surfaces of the parts and in view of their low cost, each specimen was tested only once and test replications were performed on new pieces.
2. *Cylindrical fits*. The cylindrical fit in Fig. 5b, fabricated in 33 samples, includes a ∅16 mm steel pin (head and shank of a commercial M16 hexagonal bolt of grade 8), a square (40 × 15) steel clamp (steel C40 to EN 10083-2) and a transverse commercial M8 steel screw (grade 12.9). The clamp receives the pin in a centre hole (∅16 mm) and is made flexible by a through radial slot, perpendicular to the screw axis. The parts were prepared by manual sanding the cylindrical surfaces of pin and clamp with emery paper (grit size P60), degreasing with liquid trichloroethane and smearing with lubricating paste (Molykote G-n plus) the threads and the bearing head surface of the transverse screw. Lubrication aimed at achieving a low (about 0.05) and repeatable frictional coefficient throughout the tests. After application of the adhesive (if any) to the cylindrical surfaces, the pin was inserted into the hole of the clamp and the parts were tightened at the requested torque by means of the transverse screw. The clamping force on the pin can be related to the tightening torque on the screw by means of textbook formulae. The strength measurements were made by recording with an electronic wrench the torque needed to break the interface under twist. The hexagonal head of the pin and the square outline of

the clamp helped in fitting the parts to the wrench and to a vice during this operation. To avoid stressing of the interface under the closing force of the vice, the test pieces were held at the bottom of the vertical sides (Fig. 5b) so that the force line ran within the metal ligament opposite to the tightening screw. Although regeneration of the working surfaces would have been possible after testing, in the present experimental campaign each of the 33 specimens was used only once.

3. *Double-lap joints*. The double-lap joint in Fig. 5c, manufactured in eleven pieces, is composed of two hollow steel (C40 to EN 10083-2) discs (∅14 × 50 × 15 mm), three peripheral steel (C40 to EN 10083-2) cylinders (∅20 × 10), a commercial (M14 × 60) centre steel bolt (grade 12.9), a hardened steel washer (HRC = 60) and a commercial (M14 × 12) steel nut (grade 10). The specimens were prepared by manual sanding the flat surfaces of discs and cylinders with emery paper (grit size P60), degreasing all parts by repeated soaking in liquid trichloroethane and smearing bolt and nut threads with lubricating paste (Molykote G-n plus). Upon assembly, the three cylinders (each of exactly the same height) were interposed between the (coaxial) discs in such a way that their centres lay on the rim of the discs with 120° angular spacing. The equal thickness and the regular spacing ensured an equal share among the cylinders of the axial preload imposed on the bolt by a controlled torque. The adhesive (if any) was applied to the bases of each cylinder prior to formation of the specimen. The strength measurements were made by recording the maximum load (applied by a hydraulic testing machine) needed to displace radially by a small amount (1 mm) each cylinder with respect to the discs. In this way, each specimen supplied three readings involving the same assembly conditions. The surfaces of discs and cylinders were regenerated once (and the parts tested a second time) by chemical removal of cured adhesive residuals and mechanical flattening on a plane grinding machine.

The real joints tested by Dragoni and Mauri [8] were bonded with adhesives Loctite 638 and 243, the most representative products (in commercial terms) within the categories of high- and medium-strength anaerobics of the Loctite product range. A number of unbonded joints were again included in each test run so as to establish a reference baseline for the strength values at different levels of the contact pressure.

2.3 Fatigue Strength

Fatigue failures in the mating parts of a clamped connection are a common occurrence in mechanical constructions. Although the degradation of rubbing surfaces (fretting) is often a stimulus to fracture initiation [6, 13], these failures can be classified as a stress concentration problem [31] and is well documented in the technical literature (see [15] for the shaft-hub connection).

The work by Dragoni [9] examined the intimate strength of the interface (be it dry, slip bonded or hybrid) which represents the weakest link of the joint once classical stress concentrations have been eliminated. In order to achieve failure at the interface and gain information on its properties, the test specimens shown in Fig. 6 were adopted. The specimen comprises a tapered (1:50) pin (∅10 × 30 mm) and a collar (∅10 × 30 × 9 mm) with tapered (1:50) center hole. The pin is a commercial item made of alloy steel, hardened to $S_u = 1.500$ N/mm^2 and ground on the conical surface. The collar, obtained by cutting, boring and reaming a ground round bar, is made of carbon steel, quenched and drawn to $S_u = 800$ N/mm^2. The specimen dimensions are similar to those prescribed for cylindrical pin and collars by ISO 10123, the main standard addressing the static strength of anaerobics. Cylindrical specimens of this type (pin ∅12.7 × 50 mm, collar ∅12.7 × 25.4 × 11 mm, both of mild steel) were used in Dragoni's [9] work (see below) for exploratory fatigue tests on slip bonded (no interference) assemblies.

Use of tapered specimens for systematic fatigue testing has many advantages: inexpensive fabrication and easy preparation of the parts (Fig. 6a); simple adjustment of the contact pressure through control of the axial push-on force (Fig. 6b); straightforward axial loading by push-off compression on reverse (Fig. 6c); certain accomplishment of failures at the interface; clear detection of failure by neat ejection of the pin from the collar. The main limitation of the specimens lies in the irregularity of the contact pressure (upon assembly) and of the shear stress (upon loading) over the interface, including singularities at the edges of the contact [1]. As a consequence, although significant for real joints with the same proportions as the specimens, the measured strength values are probably lower than the true properties of the interface.

Dragoni [9] manufactured the specimens in homogeneous batches of 30 (cylindrical specimens) and 100 samples (tapered specimens), all showing a roughness of the mating surfaces in the range $Ra = 1.2$–1.6 μm. Before assembly, the parts were cleaned by repeated soaking in liquid trichloroethane followed by wiping with cotton cloth and final drying (solvent evaporation under hood cabinet). When applicable, the parts were bonded with the anaerobic adhesive Loctite 638, the high grade retaining product used extensively in the static testing of the previous sections. The tests were performed according to a factorial scheme which

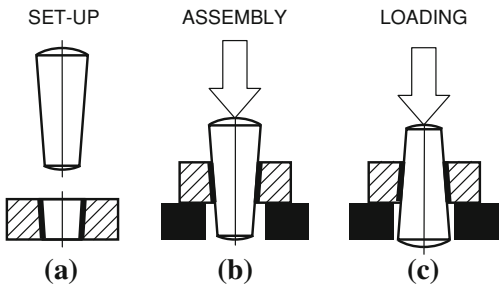

Fig. 6 Geometry of the tapered specimen for fatigue testing showing set-up (**a**), assembly (**b**) and loading arrangements (**c**). *Bondline* shown with *heavy lines*

combined in all relevant ways the three following experimental factors, each variable over two levels: set-up, dry (no adhesive) or bonded (Loctite 638); assembly, slip fit (no contact pressure) or press fit (mean pressure of about 150 N/mm^2); loading, quasi-static (monotonic) or fatigue (repeated stress).

The coefficient of friction, needed to convert the axial assembly force into (mean) contact pressure, was retrieved (for both dry and adhesive joints) from two parameters. One parameter was the slope of the force–displacement diagram recorded at assembly. The second parameter was the ratio between maximum assembly force and corresponding hoop strain in the collar as captured by an electrical-resistance strain gauge applied on the outer surface (see Sect. 3.3). Elaborated by means of the formulas for taper connections and thick-walled cylinders [9], the above parameters provided the coefficient of friction between the parts.

The fatigue tests were carried out under cyclic loading (stress ratio $R = F_{min}/F_{max} = 1/19$) at a constant frequency of 110 Hz. The load was applied axially to the thinner end of the pins as shown in (Fig. 6c). Despite the high frequency, Dragoni [9] detected no appreciable temperature increase in the adhesive. The criteria adopted to terminate the single fatigue test were either the achievement of joint failure (testified by gross disengagement of the pin) or the attainment of a fatigue life of 10 million cycles (run-out). The fatigue limit was identified using a reduced form of the staircase method [5, 22]. For one run-out (within each specimen type) that had survived the maximum stress amplitude, loading was prolonged to either failure or completion of 200 million cycles. The other survived specimens were fractured statically and the residual ultimate strength was recorded.

3 Experimental Results

3.1 Static Strength of the Ideal Interface

Figure 7 shows the typical relationship between applied torque and twist angle measured at breakaway of friction and hybrid interfaces. The assembly contact pressure was 150 N/mm^2 in both cases and the hybrid interface was bonded with Loctite 638 [7]. The curves were obtained by means of an electronic wrench fitted with an encoder for measuring the rotation angle of bushing 4 with respect to the vice fastening bushing 5 (see Fig. 3). Slopes *OA* and *OB* of the curves in Fig. 7 reflect the behaviour of the rig (comprising take up of backlashes and elastic deformation) up to yielding of the interface (peaks *A* and *B*). After achieving the peak values, both curves exhibit a drop. For the purely friction interface, the drop is due to switching from static to sliding friction. For the hybrid interface, it is consequent upon failure of the adhesive bonds. By increasing rotations, the residual strength of the hybrid interface remains stationary, whereas that of the

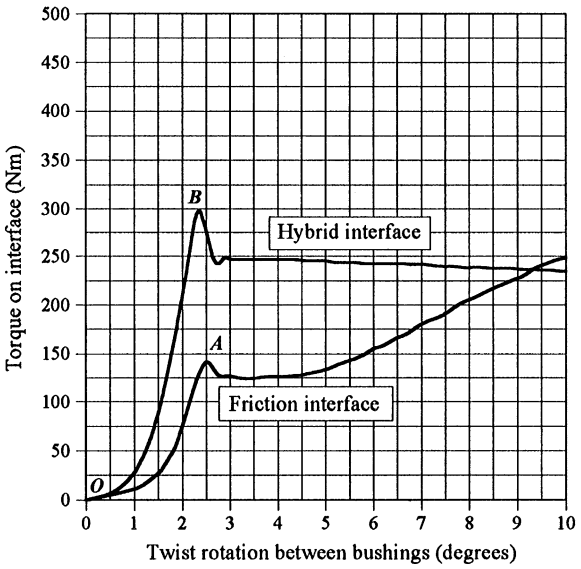

Fig. 7 Relationship between applied torque and relative twist of bushings 4 and 5 in the device of Fig. 3 (adhesive = Loctite 638; contact pressure = 150 N/mm^2; [7]

friction interface grows steadily. Close observation of the unbonded surfaces after the test spotted large areas of galling, which explains such an increase. Output curves as in Fig. 7 were collected for several preliminary trials showing a quite reproducible response. In the actual tests, only the peak torque values (*A* or *B*) encountered anywhere during a bushing rotation of about 4° was recorded by the wrench.

For the product Loctite 638, Fig. 8 presents the results by Dragoni and Mauri [7] in terms of ultimate shear strength (vertical axis) plotted against the mean contact pressure (horizontal axis). It is seen that the strength of both bonded (solid circles) and unbonded (hollow circles) interfaces steadily builds up linearly with the contact pressure and that the slopes of the two interpolating lines are almost the same (about 0.17). For any given contact pressure, the cumulative strength of the hybrid interface can thus be calculated by adding the strength of the purely adhesive interface (about 28 N/mm^2 at zero contact pressure) to the strength of the purely frictional interface at that particular pressure. This result is consistent with the physical explanation that the adhesive is squeezed out from the small spots where the crests of the mating rough surfaces touch each other and is accumulated in the relatively larger surrounding volumes. According to this model, the intermetallic junctions provide the same frictional strength (proportional to the contact pressure) as in the dry joint, while the surrounding adhesive bonds provide a strength contribution (independent from the pressure) equal to that of the adhesive alone.

However, when the strength of hybrid interfaces bonded with other anaerobic adhesives is considered [8] a different picture emerges. Figure 9 collects the strength results from all the adhesives tested by Dragoni and Mauri [7, 8] under ideal conditions. Superimposed on the data for Loctite 638 (solid circles) and for

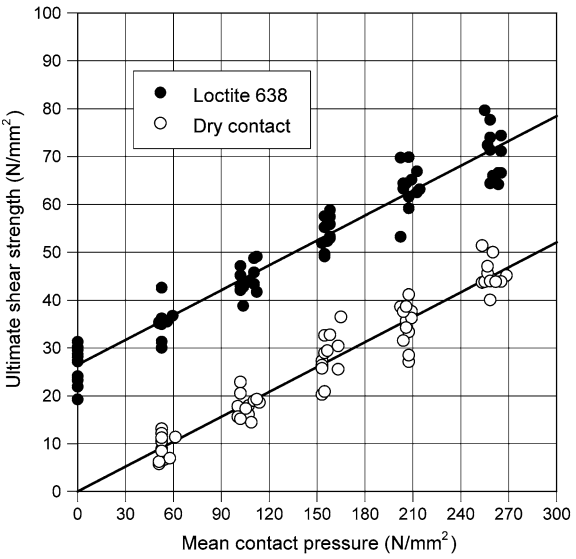

Fig. 8 Static strength of a strong anaerobic (Loctite 638) and of dry contact measured under ideal conditions with the device in Fig. 3 [7]

the unbonded interface (dashed line), already shown in Fig. 8 [7], displayed in Fig. 9 are also the results for products Loctite 601, 243, 242, and 222 [8]. Figure 9 confirms that the cumulative strength of all bonded interfaces steadily increases with the applied contact pressure, but the rate of the build-up is not the same for all products. For the adhesives Loctite 243 (examined under four pressure levels) and 601 (examined under three pressure levels) the increase is also remarkably linear. For the adhesives 222 and 242, nothing can be said on linearity since the only available data involve the maximum pressure (260 N/mm^2) deliverable by the

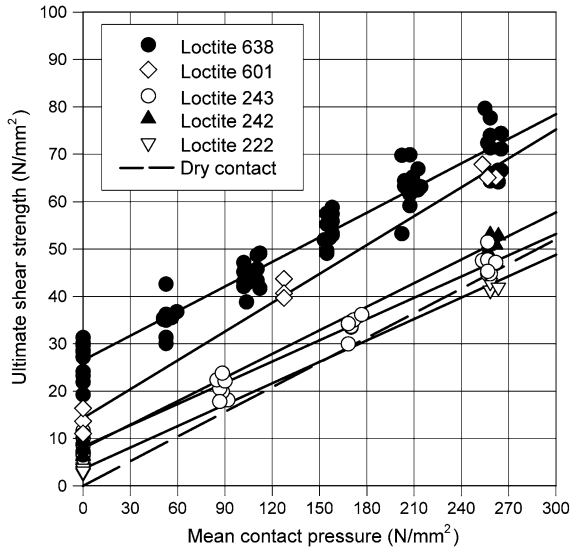

Fig. 9 Static strength of several anaerobics and of dry contact measured under ideal conditions with the device in Fig. 3 [8]

equipment in Fig. 3 or no pressure at all. Although the trend of adhesive 242 (solid triangles) and 638 (solid circles) exhibit the same slope characterising the strength of the unbonded interface (dashed line), different strength gradients than the dry parts are displayed by the interfaces formed with adhesive 601 (steeper slope) and adhesives 243 and 222 (flatter slope). In the case of product 222, the line of the bonded interface crosses over that of the dry interface within the range of contact pressures examined. Overall, the observed behaviour cannot support the superposition criterion surmised above and calls for a different interpretation (see Sect. 4).

3.2 Static Strength of Real Joints

The strength results for the real joints of Fig. 5 are collected in Fig. 10 (threaded connection), Fig. 11 (cylindrical fit) and Fig. 12 (double-lap joint). Unlike Figs. 8 and 9, where the local parameters (contact pressure and shear strength) of the interface are plotted, Figs. 10, 11, 12 display the macroscopic properties of the joints (preload or tightening torque on the horizontal axis and breakaway force or torque on the vertical axis). The choice is due to the uneven working conditions over the real interfaces, particularly irregular in terms of contact pressure, that spoil the meaning of local variables (compare, for instance, the pressure between active and inactive flanks of the engaging threads in the bolted joint in Fig. 5a). Figures 10, 11, 12 provide both the individual experimental points (different symbols in relation to the particular interface) and the linear regressions (straight

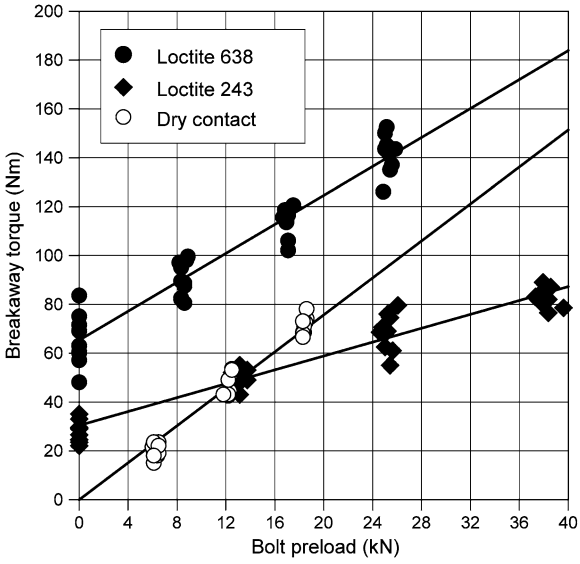

Fig. 10 Static strength under different bonding conditions of the threaded connections in Fig. 5a [8]

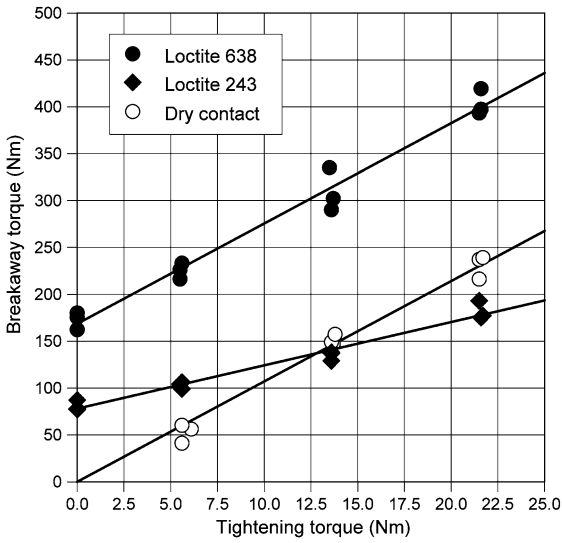

Fig. 11 Static strength under different bonding conditions of the cylindrical fits in Fig. 5b [8]

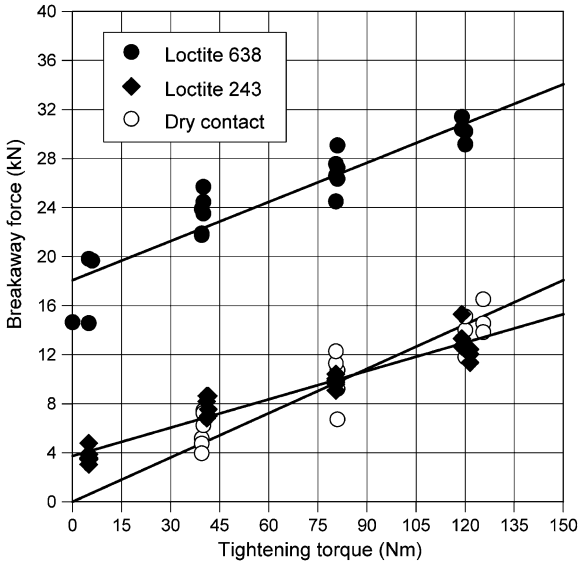

Fig. 12 Static strength under different bonding conditions of the double-lap joints in Fig. 5b [8]

lines) of each family of interfaces. For the dry joints, the interpolating lines were forced to start from the origin.

The data for the threaded connections (Fig. 10) derived from a total of 110 tests, parted in two runs of 55 fresh (not recycled) samples. Each run comprised eleven assembly conditions (four pressure levels for the bonded joints and three levels for the unbonded joints) with five repetitions. The preloads appearing in Fig. 10 were calculated from the tightening torques actually applied to the

specimens during the tests. The conversion is needed because of the different frictional coefficients affecting the three interfaces (unbonded and bonded with Loctite 243 or Loctite 638) during tightening, when the two adhesives behave as (dissimilar) lubricants with respect to the dry contact. The relationship between torque and preload was measured directly on several specimens, modified by replacing the lower nut (Fig. 5a) with an annular load cell. The details on the torque-preload conversion procedure are provided by Dragoni and Mauri [8]. The conversion explains the different range of preloads covered by the experimental points in Fig. 10, originated by different frictional coefficients between threads in response to fixed torque levels applied to the upper nut in Fig. 5a. No such conversion was required for the cylindrical fits (Fig. 5b) and the double-lap joints (Fig. 5c). Supplied by an independent bolt, in both cases the contact force is proportional to the tightening torque through a constant (though unknown) coefficient irrespective of the particular working conditions at the active interface.

The strength data of the cylindrical fits (Fig. 11) embrace a total of 33 tests, performed on a single batch of all available samples. The batch included eleven assembly conditions (four pressure levels for both bonded joints and three for the dry joint) with three replications.

The results for the double-lap joints (Fig. 12) were obtained from two batches of eleven specimens (all available rigs shown in Fig. 5c). Each batch encompassed eleven different assembly conditions (four pressure levels for both bonded joints and three for the dry joint) with three repetitions (the three small cylinders) per assembly.

As for the ideal interface (Figs. 8, 9), the behaviour of the real joints in Figs. 10, 11, 12 indicated a similarity between the dry joints and the joints bonded with Loctite 638 in terms of strength build-up with the contact pressure. Likewise, the characteristic lines of the joints bonded with Loctite 243 show (more markedly than the ideal interface) a lower gradient than that of the dry joint. Though sensitive to the contact pressure, the strength of product 243 intersects that of the dry parts in the range of measurements for all three real couplings. Again, the simple model based on the superimposition of dry friction strength and adhesive strength fails to predict the cumulative strength of the hybrid joints, especially if bonded with a medium-strength anaerobic (Loctite 243). A micromechanical model describing the observed macroscopic behaviour of the hybrid interface, regardless of the bonding adhesive used, is proposed in Sect. 4.

3.3 Fatigue Strength

Figure 13 provides an example of the force–displacement diagram at insertion of the pin into the collars (see Fig. 6b). The ratio $\Delta F/\Delta s$ in Fig. 13 measures the slope of the linear steady-state portion of the diagram that follows the nonlinear run-in arc. Using $\Delta F/\Delta s$ and the equations for thick-walled taper fits, Dragoni [9] calculated the coefficient of friction and the mean contact pressure between pin and

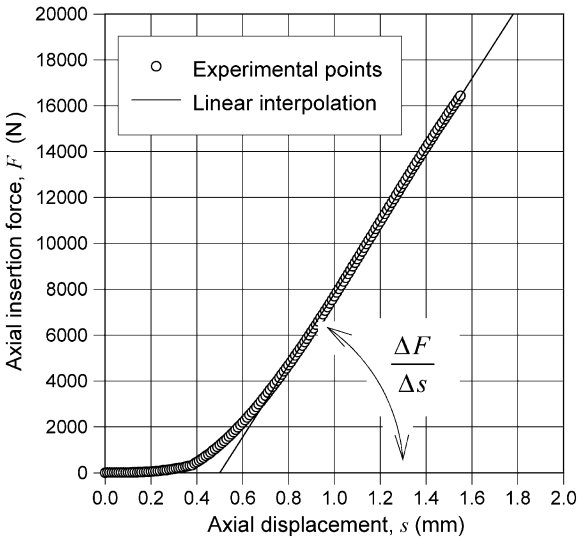

Fig. 13 Typical plot of insertion force against axial displacement at assembly for the tapered specimen in Fig. 6 [9]

collar for each joint. As an alternative, the friction coefficient was also calculated by measuring the circumferential expansion of the outer surface of the collar by means of electrical-resistance strain gauges (Fig. 14).

Figure 15 displays an assortment of tapered specimens after test, comprising a dry press fit (Fig. 15a), a bonded slip fit (Fig. 15b) and a bonded press fit (Fig. 15c). It is seen that, according to expectations, all specimens failed neatly at the interface, without any sign of damage in the mating parts.

The results by Dragoni [9] derived from the reference static tests on bonded and unbonded taper press fits are displayed in Fig. 16, which plots the ultimate unit shear strength against the mean contact pressure. The unit shear strength is simply

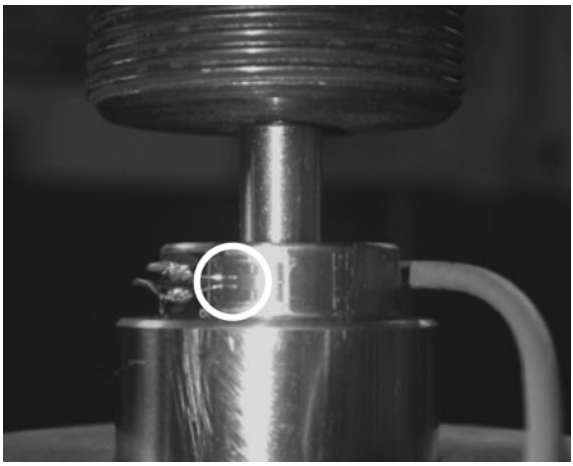

Fig. 14 Close-up of a tapered specimen during assembly showing the collar instrumented with an electrical-resistance strain gauge (*circled*)

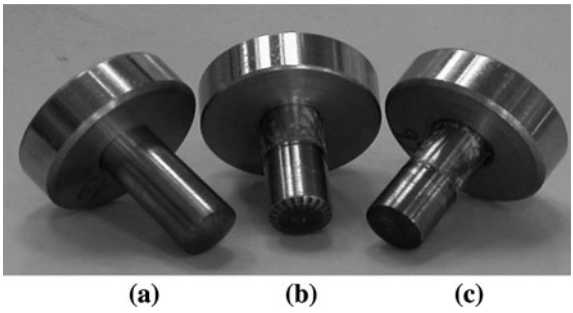

Fig. 15 Tapered pin-collar specimens after testing: **a** dry press fit, **b** bonded slip fit, **c** bonded press fit

given by the ratio of the ultimate load over the area of engagement (291 mm^2) between pin and collar. In Fig. 16, the linear interpolations for both dry and bonded joints are superimposed (solid lines) on the set of experimental points (circles). For the dry joints, the origin is used as a virtual point since no contact pressure implies no mechanical strength. Figure 16 supports the main finding of the previous section that the static strength increases with the contact pressure but with different gradients for dry and bonded joints. The heuristic principle of superimposition of effects (independent action of friction and adhesive) is again negated as a rational tool for calculating the static strength of the hybrid joint.

Also addressing specific quantities (unit shear strength and contact pressure), Fig. 17 contrasts the static strength (solid lines) with the (mean) fatigue strength (dashed lines) measured in the tests by Dragoni [9]. The values of the fatigue strength correspond to the loading amplitude at the 50% of probability of failure. The static strength results (taken from Fig. 16) are accompanied by the confidence interval (plus or minus one standard deviation). The scatter is not provided for the

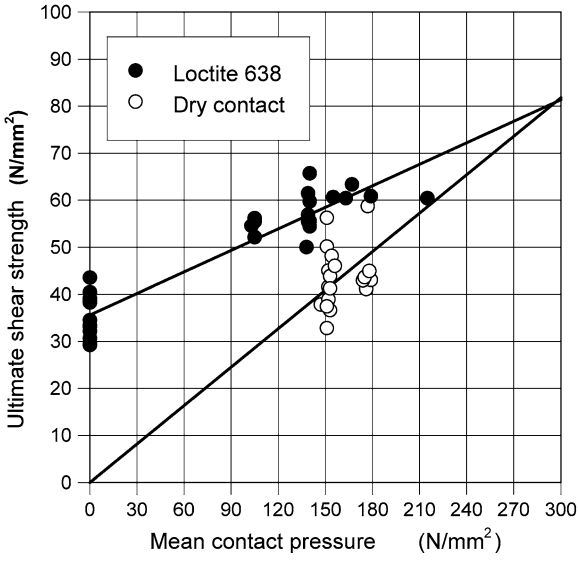

Fig. 16 Variation of ultimate shear strength with contact pressure for dry and bonded taper fits of Fig. 6 [9]

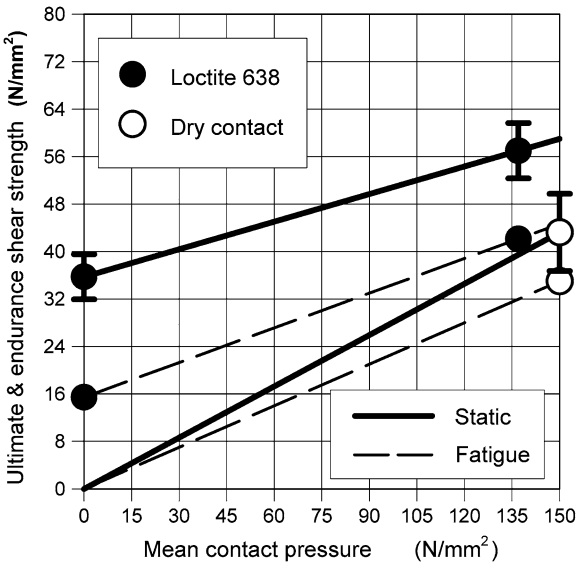

Fig. 17 Comparison between static and fatigue strength for dry and bonded taper fits [9]

fatigue strength results because the reduced staircase method adopted does not supply it [5]. The high scatter affecting the response of the dry press fits can be explained by the uncertainty that accompanies the friction forces between unlubricated metals.

Most interesting in Fig. 17 is the comparison of the fatigue strength with the static strength, from which distinct behaviors for dry and bonded joints emerge. The fatigue strength of the bonded specimens (dashed line with end solid circles) shows a definite decay with respect to the static strength. In absolute terms, the decay is approximately independent of the contact pressure and equals roughly one half of the static strength of the adhesive alone. This observation suggests a simple rule that can be usefully applied in design practice (as far as a life of 10 million cycles is concerned).

In comparison to Fig. 17, the fatigue tests of Croccolo et al. [4] indicate that when exposed to cyclic loading fluctuating from the static strength with amplitude of one half the adhesive strength, bonded press fits lose entirely their retaining capacity. This lower performance can be explained with the adhesive filling less efficiently the interface in the cylindrical press fits by Croccolo et al. [4] than in the taper fits by Dragoni [9].

When the attention is moved in Fig. 17 to the fatigue strength of the dry joints, quite another conclusion is drawn. First of all, it must be remarked that all failures taking place in this case occurred at the launch of the test with the specimens not even undergoing the very first load cycle. In fact, the failures were of static nature and the fatigue tests were actually static tests performed with the (reduced) staircase method. All specimens that could survive the first load cycle also survived the chosen threshold life of 10 million cycles. From this outcome it can be surmised that the dry interface is virtually unaffected by fatigue damage.

This explains why the fatigue data point of the dry press fits in Fig. 17 falls almost within the scatter interval of the static strength for the same joint. The difference between the mean values of the two strengths can be explained by the fact that the static and the fatigue data derive from sets of specimens prepared and tested separately from each other.

Dragoni [9] also reports that the residual static strength of the dry press fits surviving the fatigue testing coincides with that of the fresh joints. By contrast, a decay of the residual static strength affected the bonded joints which survived fatigue testing (10 million cycles), an indication of the absence of a true fatigue limit for the category of bonded press fits. This speculation is corroborated by the behavior of the run-outs (one for each type of fit) for which the fatigue loading was prolonged beyond the threshold of 10 million cycles. The run-outs dry press fit endured a life of 200 million cycles with no signs of failure (after which the testing was terminated). By contrast, the two bonded specimens failed after a (total) life of 90 million cycles (slip fit) and of 105 million cycles (press fit). Whether a true fatigue limit for bonded slip fits and bonded press fits actually exists remains an open question and represents a fruitful topic for future research.

4 Joint Modelling

4.1 Micromechanical Model of the Hybrid Interface

Consider the simple model depicted in Fig. 18a of a hybrid interface between two massive adherends, bonded and tightened under the normal force P. In Fig. 18a the roughness of the contacting surfaces has been condensed into two protrusions

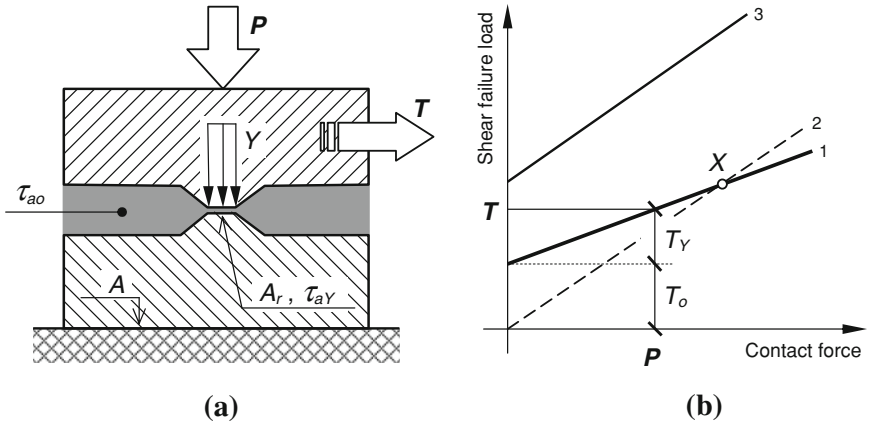

Fig. 18 Micromechanical model of the hybrid interface (**a**) and corresponding predictions (**b**) for its macroscopic shear strength [8]

that touch each other over a fraction, A_r, of the nominal contact area, A. It is also assumed that the adhesive fills the voids surrounding the protrusions, where it sustains no pressure, and forms a thin layer between the protrusions, subjected to the yield pressure, Y, of the softest adherend [10].

In order to break the joint, the area, A_e ($= A - A_r$), of the adhesive around the asperities and the area, A_r, of the adhesive entrapped between the asperities must be fractured. For very stiff adherends (as typical of anaerobics) loaded statically, those areas are likely to break simultaneously. If τ_{ao} is the unit shear strength of the adhesive at zero pressure and τ_{aY} the shear strength of the adhesive at pressure Y, the shear failure load, T, of the joint amounts to

$$T = \tau_{ao} A_e + \tau_{aY} A_r = \tau_{ao} (A - A_r) + \tau_{aY} A_r \tag{1}$$

From the equilibrium condition of each adherend in the vertical direction, $YA_r = P$, the true area of contact, A_r, is calculated as

$$A_r = P/Y \tag{2}$$

Combination of (1) and (2) followed by some rearrangements yields

$$T = \tau_{ao} A + (\tau_{aY} - \tau_{ao}) P / Y = T_o + T_Y \tag{3}$$

Equation (3) shows that the macroscopic strength of the joint, T, is the sum of a constant term, $T_o = \tau_{ao} A$, and a variable term, $T_Y = [(\tau_{aY} - \tau_{ao})/Y] P$, proportional (whenever $\tau_{aY} > \tau_{ao}$) to the contact force. This produces the generic diagram of Fig. 18b (curve 1).

For a dry joint ($\tau_{ao} \equiv 0$, $\tau_{aY} \equiv \tau_Y =$ shear strength of the metal junctions), Eq. 3 predicts $T_o = 0$ and $T_Y = (\tau_Y/Y) P$ in accordance with Coulomb's law (Fig. 18b, curve 2).

For a bonded joint where the adhesive would be squeezed out of the junctions upon tightening ($\tau_{aY} \equiv \tau_Y \gg \tau_{ao}$), Eq. 3 would predict the same constant term $T_o = \tau_{ao} A$ as in the purely adhesive joint and a variable term $T_Y = [(\tau_Y - \tau_{ao})/Y] P \approx (\tau_Y/Y) P$ with the same slope as the dry joint. This is the rationale behind the criterion of superimposition of effects, stated in the Introduction and recalled throughout the paper, that must be dismissed on experimental grounds.

A possible explanation of the experimental results is that a thin film of adhesive is actually formed between the crests of the matching surfaces. According to a mechanism well documented for polymers [20] and adhesives [18, 26], under the high local pressure (Y) this film could achieve a shear strength (τ_{aY}) significantly greater than the shear strength at no pressure (τ_{ao}). According to this interpretation, it would be expected that the higher the strength at zero pressure (τ_{ao}), the higher the strength (τ_{aY}) under the yield pressure of the adherends, hence the higher the slope, $(\tau_{aY} - \tau_{ao})/Y$ in Eq. 3, of the characteristic curve in response to the clamping force (Fig. 18b, curves 1 and 3). Observation of Figs. 8, 9, 10, 11, 12 indicates that this is the case, with the stronger anaerobic (Loctite 638) outperforming the medium one (Loctite 243) in both respects (greater strength at zero pressure and greater strength gradient under pressure). When a weak anaerobic is

used (low value of $\tau_{aY} - \tau_{ao}$ in Eq. 3), the slope of the characteristic line for the hybrid interface becomes lower than the slope for the dry joint and the two curves cross each other (point X in Fig. 18). In this case, the adhesive between the crests of the roughness behaves as a solid lubricant.

The proposed micromechanical model points out the role of the shear strength of the pressurised adhesive for the rational characterisation of the hybrid interface under steady stresses. Research aimed at confirming this mechanism would help understanding the intimate behaviour of these joints and would also give directions for the development of new adhesives tailored to specific applications.

4.2 Strength Calculation of Actual Joints

Although elaborate models exist for the stress distribution at the interface of hybrid adhesive–friction joints [14, 25, 32–34] their usefulness for actual strength prediction are very limited. This is because the formulae are quite elaborate and because the geometries examined so far are essentially restricted to pin and collar engagements under axial or torsional loading.

By assuming that the metal adherends are rigid (not deformable) and that the hybrid interface behaves as an elastically deformable layer, the strength of the joint can be estimated with elementary strength of material models. Although extreme, the above assumption leads to simple equations, easy to use and accurate enough for most engineering problems.

This section presents the strength equations for five common geometries of hybrid friction–adhesive joints: (1) threaded connection, (2) overlap joint, (3) cylindrical fit, (4) taper fit, (5) flanged coupling. For all equations, the joint type and dimensions are defined in Fig. 19a–e and the following material properties are used:

τ_{ao} = static shear strength of the adhesive (e.g. measured on pin-collar slip fits)
τ_T = cumulative static shear strength of the hybrid interface (measured on hybrid joints under the same contact pressure as the final joint)

1. Threaded connection (Fig. 19a)
   Maximum axial force: $F =$ not applicable
   Maximum torque: $M_t = (\tau_{a0} + \tau_T)\pi H(D - 0.65\,a)^2 + 0.65 f\,VD$ where a is the pitch of the thread (to ISO 68), V is the preload in the screw and f is the coefficient of friction between nut and plate.
2. Overlap joint (Fig. 19b)
   Maximum axial force: $F = \tau_T A$
   Maximum torque: $M_t =$ not applicable
3. Cylindrical fit (Fig. 19c)
   Maximum axial force: $F = \tau_T \pi DL$
   Maximum torque: $M_t = \tau_T \frac{\pi D^2 L}{2}$

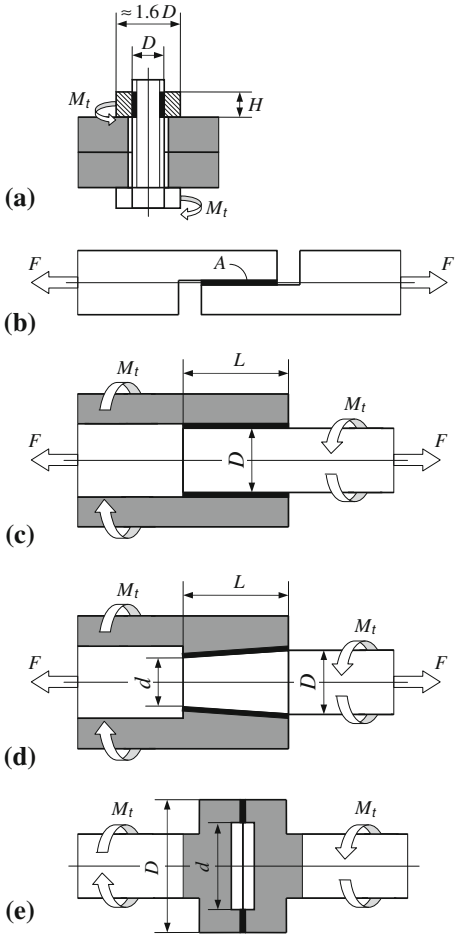

Fig. 19 Typical configurations of hybrid friction–adhesive joints encountered in engineering practice: **a** threaded connection, **b** overlap joint, **c** cylindrical fit, **d** taper fit, **e** flanged coupling

4. Taper fit (Fig. 19d)

   Maximum axial force: $F = \tau_T \frac{\pi(D+d)\sqrt{(D-d)^2+4L^2}}{4}$ (use only if $D - d \leq 0.3L$)

   Maximum torque: $M_t = \tau_T \frac{\pi(D+d)\left[(D+d)^2-2dD\right]\sqrt{(D-d)^2+4L^2}}{16D}$

5. Flanged coupling (Fig. 19e)

   Maximum axial force: $F =$ not applicable

   Maximum torque: $M_t = \tau_T \frac{\pi\left(D^4-d^4\right)}{16D}$

Use of the above equations is reliable for the prediction of the static strength of the joints. Due to the uncertainty of fatigue data, adaptation to cyclic loading should be performed with care. For example, based on the fatigue results presented in Sect. 3.3, the cyclic strength under repeated stresses can be estimated by replacing τ_{ao} with $0.5\tau_{ao}$ and τ_T with $\tau_T - 0.5\tau_{ao}$.

5 Conclusions

Anaerobic adhesives (anaerobics) are a simple and very effective means of enhancing the performance of classical friction joints in which retaining forces are promoted by mechanical tightening. Entrapped in the airless environment arising between closely mating machinery parts, anaerobics cure thanks to intimate contact with active metals (for example iron and copper) and to the absence of oxygen. Advantages of anaerobic-augmented friction joints are extra sealing action, lower fretting wear, better corrosion resistance, greater stiffness and higher mechanical strength. These benefits can be achieved with minor or no changes to the design of the parts with respect to the classical assembly. This chapter has reviewed the literature on friction–adhesive joints with the focus on their mechanical strength, both static and fatigue. Data were gathered from experiments on ideal interfaces (annular butt joints under uniform stress conditions) and actual joint geometries (threaded connections, cylindrical and taper fits, double-lap joints under realistically irregular stresses). The results can be summarised as follows:

- the overall static strength of both dry (friction only) and hybrid joints (friction and adhesive) steadily builds up with the contact pressure (clamping force),
- the static strength build-up of the joints bonded with strong anaerobics (retainers) is similar to that of the dry joint (same strength rate with contact pressure),
- when low- or medium-strength anaerobics (i.e. threadlockers) are used, the static strength build-up is much lower in the hybrid than in the dry joint,
- for high contact pressures, the dry joint can achieve a mechanical strength much higher than the joint bonded with low- or medium-strength anaerobics (solid lubrication),
- predicting the cumulative static strength of the hybrid joint as the sum of adhesive strength and friction strength, calculated independently from each other, can result in gross errors,
- the fatigue strength of all joints (dry and bonded) increases with the contact pressure induced at assembly,
- the fatigue strength of the dry joint is comparable to its static strength at equal pressure,
- the fatigue strength of the bonded joint is significantly lower than its static strength; the decay seems to be independent (in absolute terms) of the contact pressure.

A micromechanical model explaining most of the experimental evidence was presented which spurs further research for the correct interpretation of the basic mechanisms underlying this hybrid joining technology. Simple equations were provided to help the designer predict the strength of virtually all types of friction–adhesive joints occurring in engineering applications.

References

1. Akisanya, A.R.: On the singular stress field near the edge of bonded joints. J. Strain Anal. **32**, 301–311 (1997)
2. Bartolozzi, G., Croccolo, D., Chiapparini, M.: Research on shaft-hub adhesive and compression coupling. ÖIAZ **144**, 198–201 (1999)
3. Canyurt, O.E.: Fatigue strength estimation of adhesively bonded tubular joint using genetic algorithm approach. Int. J. Mech. Sci. **46**, 359–370 (2004)
4. Croccolo, D., De Agostinis, M., Vincenzi, N.: Static and dynamic strength evaluation of interference fit and adhesively bonded cylindrical joints. Int. J. Adhes. Adhes. **30**, 359–366 (2010)
5. Dixon, W.J., Massey, Jr F.J.: Introduction to Statistical Analysis, 4th edn, pp 434–438. McGraw-Hill, New York (1985)
6. Dragoni, E.: Effect of anaerobic threadlockers on the fatigue strength of threaded connections. Int. J. Mat. Prod. Technol. **14**, 445–455 (1999)
7. Dragoni, E., Mauri, P.: Intrinsic static strength of friction interfaces augmented with anaerobic adhesives. Int. J. Adhes. Adhes. **20**, 315–321 (2000)
8. Dragoni, E., Mauri, P.: Cumulative static strength of tightened joints bonded with anaerobic adhesives. Proc. Inst. Mech. Eng. Part L **216**, 9–15 (2002)
9. Dragoni, E.: Fatigue testing of taper press fits bonded with anaerobic adhesives. J. Adhes. **79**, 729–747 (2003)
10. Halling, J.: Principles of Tribology. McMillan, London (1975)
11. Harrigan, T.P., Kareh, J.E., Harris, W.H. (1990) The influence of support conditions in the loading fixture on failure mechanisms in the push-out test: a finite element study. J. Orthop. Res. **8**, 678–684 (1975)
12. Haviland, G.S.: Machinery Adhesives for Locking Retaining and Sealing. Marcel Decker, New York (1986)
13. Hoeppner, D.W., Chandrasekaran, V., Elliot, C.B.: STP 136—Fretting fatigue: current technology and practices. ASTM (2000)
14. Kawamura, H., Sawa, T., Yoneno, M., Nakamura, T.: Effect of fitted position on stress distribution and strength of a bonded shrink fitted joint subjected to torsion. Int. J. Adhes. Adhes. **23**, 131–140 (2003)
15. Kollmann, F.G.: Welle-Nabe-Verbindungen. Gestaltung, Auslegung, Auswahl. Springer, Berlin (1984)
16. Liechti, K.M., Hayashi, T.: On the uniformity of stresses in some adhesive deformation specimens. J. Adhes. **29**, 167–191 (1989)
17. Mahon, F.: Use of anaerobic adhesives to enhance strength and capacity of flanged couplings. Paper 950125, SAE Intl Congress and Exposition, Detroit, 27th February–2 March (1995)
18. Mengel, R., Haeberle, J., Schlimmer, M.: Mechanical properties of hub/shaft joints adhesively bonded and cured under hydrostatic pressure. Int. J. Adhes. Adhes. **27**, 568–573 (2007)
19. O'Reilly, C.: Designing bonded cylindrical joints for automotive applications. Paper 900776, SAE Intl Congress and Exposition, Detroit, 26th February–2nd March (1990)
20. Raghava, R.S., Cadell, R.M.: The macroscopic yield behaviour of polymers. J. Mater. Sci **8**, 225–232 (1973)
21. Renton, W.J.: The symmetric lap shear test—what good is it? Exp. Mech. **16**, 409–415 (1976)
22. Rice, R.C.: Fatigue data analysis. In Metals Handbook: Mechanical Testing, vol. 8, pp. 703–704. American Society for Metals, Metals Park, Ohio (1985)
23. Romanos, G.: Strength evaluation of axisymmetric bonded joints using anaerobic adhesives. Int. J. Mat. Prod. Technol **14**, 430–443 (1999)
24. Sawa, T., Sasaki, R., Yoneno, M.: An analysis of pipe flange connections using epoxy adhesives/anaerobic sealant instead of gaskets. ASME J. Press Vessel Technol. **117**, 298–304 (1995)

25. Sawa, T., Yoneno, M., Motegi, Y.: Stress analysis and strength evaluation of bonded shrink fitted joints subjected to torsional loads. J. Adhes. Sci. Technol. **15**, 23–42 (2001)
26. Schlimmer, M.: Anstrengungshypothese für Metallklebverbindungen. Materialwissenschaft und Werkstofftechnik **13**, 215–221 (2004)
27. Sekercioglu, T., Gulsoz, A., Rende, H.: The effects of bonding clearance and interference fit on the strength of adhesively bonded cylindrical components. Mater. Design **26**, 377–381 (2005)
28. Sekercioglu, T.: Strength based reliability of adhesively bonded tubular lap joints. Mater. Design **28**, 1914–1918 (2007)
29. Sekercioglu, T., Kovan, V.: Torque strength of bolted connections with locked anaerobic adhesive. Proc. Inst. Mech. Eng. Part L **222**, 83–89 (2008)
30. Werthm, S.: (1938) Kräfte an Längspreβsitzen. VDI-Z **82**, 471–475
31. White, D.J., Humpherson, J.: Finite element analysis of stresses in shafts due to interference-fit hubs. J. Strain Anal. **4**, 105–114 (1969)
32. Yoneno, M., Sawa, T., Shimotakahara, K., Motegi, Y.: Axisymmetric stress analysis and strength of bonded shrink-fitted joints subjected to push-off forces. JSME Int. J. Ser. A **40**, 362–374 (1997a)
33. Yoneno, M., Sawa, T., Shimotakahara, K., Motegi, Y.: Push-off tests and strength evaluation of joints combining shrink fitting with bonding. Proc. SPIE **2921**, 193–198 (1997b). doi: 10.1117/12.269815
34. Yoneno, M., Sawa, T., Motegi, Y.: Axisymmetric stress analysis and strength of bonded shrink-fitted joints of solid shaft subjected to torsional loads. JSME Int. J. Ser. A **41**, 517–524 (1998)